AE MONITORING OF FATIGUE DAMAGE GROWTH IN PLAIN WEAVE COMPOSITES WITH EMBEDDED FLAWS

Jiaping Wu[1] and Ahmed Maslouhi[1]*

[1] Department of Mechanical Engineering
Université de Sherbrooke, Sherbrooke, Canada
2500 Bd Université, Faculté de genie, Sherbrooke, Québec, Canada
Jiaping.Wu@Usherbrooke.ca, Ahmed.Maslouhi@Usherbrooke.ca,
Web page: http://www.usherbrooke.ca/gmecanique/

Keywords: Fatigue damage and delamination, Acoustic emission, fatigue life curve, artificial flaws

ABSTRACT

High-modulus fibre-reinforced composites display excellent resistance to fatigue loading, but are susceptible to internal damage that can adversely alter their functional properties. Manufacturing flaws are an important limiting factor for composite application in primary structural aircraft applications. Under specific loading conditions, flaws can be originators of interlaminar damage. In service, delamination can often initiate from pre-existing manufacturing flaws [1]. Dynamic loads, the presence of interlaminar shear stresses and environmental attacks favor the propagation of delamination. Therefore, for a safe design of composite structures, it is important to understand the mechanisms of failure and essential to evaluate the effect of the presence of flaws on damage propagation and on the fatigue life.

The main objective of this study is to assess the influence of manufacturing flaws on the fatigue behaviour of plain weave composites and to evaluate experimentally the effect of environmental factors such as humidity and temperature on the fatigue life of the composite materials. Standards test coupons with an artificial delamination, created by inserting a Teflon tape which is implanted in the mid-plan of the layup, were assessed in real time by using Acoustic Emission (AE) under tension-tension cyclic loading. During mechanical cycling, the damage monitoring was supervised by using four piezoelectric sensors to catch elastic waves emitted by cracks, such as micro failures and delamination onset and growth. Therefore, a planar localization technique was applied to locate the area of damage initiation and propagation of the artificial flaw. The AE data collected during damage initiation and flaw propagation under different environmental conditions were used to generate fatigue life curves (S-N) in order to develop a predictive analytical model. This paper investigates the effect of high temperature and humidity on fatigue life of the plain weave composites. Inspection procedures such as C-scan and 3D Computed Tomography were used to evaluate the damage morphology around the artificial flaw area in the tested coupon, and the results were used to compare with damage localization results obtained by AE technique.

1 INTRODUCTION

Flaws are introduced in composite laminates in all manufacturing processes [1-6]. Typical flaws found in thermoset composites parts as a result of the manufacturing conditions are: porosity, fibre waviness, plies thermally induced cracks, micro-delamination produced by contamination and interlaminar separation induced during machining of assembly holes or impact damage [1-5]. Such flaws always lead to the formation of delamination which can become propagative when the material is subjected to dynamic loads. However, to design composite structures that are more damage tolerant, it is necessary to understand how delamination develops and how it can affect the fatigue life, the resistance, stiffness and residual performance of the structure [18]. Significant research has been performed to better understand the mechanical behavior of composites in the presence of delamination, and a large amount of literature has been published specifically on the characterization and analysis of delamination propagation in composites. However, in the published literature [7-12], the coverage of investigations associated with the effect of flaws introduced during manufacturing on

fatigue performance remains limited [13]. A reliable mechanical design of composite structures requires not only knowledge of loading conditions and safe mechanical behavior under the applied loads but also, in specific cases, also require a mechanical validation phase which must take into account the presence of flaws in the stressed structure. Therefore, in the design approach, it is necessary to integrate a damage monitoring strategy in order to characterize the growth of these flaws and to quantify the influence of their presence on the mechanical performance and on the durability of the structure. It is necessary to develop new design strategies, including exhaustive understanding of the effect of manufacturing flaws on mechanical behaviour and fatigue life of composite structures under varied loading conditions with the assistance of Structural Health Monitoring (SHM) and Non-Destructive Evaluation (NDE) [5-6]. The development of monitoring approaches for damage onset detection can help to establish reliable failure criteria that can then be used to predict fatigue life of the composite structure taking into account the growth of fabrication flaws under stressed conditions.

This study, which is a continuation of the work presented at the ICCM20 conference [13], proposes a monitoring approach to detect the initiation of fatigue damage in order to generate fatigue curves for quasi-isotropic composites containing artificial flaws. These fatigue curves will allow establishing empirical equations, which will be used to predict fatigue life [14-18] corresponding with the onset of the delamination. The main objective is to exploit AE stress wave data [9-23] to detect initiation of emerging damage in the composite under fatigue loading and to assess the effect of environmental factors such as the effect of moisture, exposure temperature and the combined influence of temperature and moisture over the fatigue behavior of the composite materials. Also, this work investigates the effect of cycling frequency over the fatigue life of the composite.

2 MATERIALS AND EXPERIMENTAL PROCEDURES

The material tested was a plain-weave (0/90) carbon/epoxy laminate prepared as a 8 plies laminates of stacking sequence $[45/0/-45/90]_S$, with coupon dimensions of 304.8 x 76.2 x 1.62 mm^3. An artificial flaw is inserted in the manufactured coupons, by embedding a centred 12.7 x 12.7 mm^2 Teflon tape between the third and the fourth layers (-45, 90). The samples were submitted to continuous tension-tension fatigue loading with AE monitoring of the coupons under constant amplitude cycling until total failure. All mechanical tests were carried out on an MTS 100 kN servo-Hydraulic testing machine under load-controlled mode. The load was transferred to the specimen through hydraulic grips, which maintained a constant pressure of 16 MPa at each extremity. Table 1 presents the number of samples used in experimental testing, and the types of environmental conditioning applied to the samples during the static and fatigue loading.

	Static testing		Fatigue testing, R=0.1							
Condition	RT*		RT		25ºC & 85%	82ºC & 85%		82ºC & Dry	120ºC & Dry	
Loading	Tension		T-T*		T-T	T-T		T-T	T-T	
Cyclic frequency	N.A		7Hz	15Hz	15Hz	7Hz	15Hz	15Hz	7Hz	
Type of sample	N.F*	W.F*	W.F	W.F	W.F	W.F	W.F	W.F	W.F	
Number of samples	6	6	5	6	9	9	9	9	10	
Maximum load (% UTL)	N.A		53, 59, 65, 71	53, 59, 65	50,55,60	50,55,60		50,55,60	50,55,60	
Damage monitoring	AE		AE	AE	AE	AE		AE	AE	

Table 1: Definition of samples, static and fatigue loading parameters and environmental conditions

Fatigue load levels were chosen by performing quasi-static tests monitored by acoustic emission at room temperature. The objective was to determine the ultimate tensile load, and the lowest loading level required to initiate damage in the composite sample. Cyclic loading levels were then chosen based upon the results from these tests. Tension-tension fatigue tests were then conducted under constant sinusoidal cycles at loading frequency of 7 Hz and 15 Hz with stress ratio R of 0.1. The assessment of the effect of the combination of high temperature exposure and moisture was achieved by testing 18 samples under 82 °C with 85% of moisture (9 samples under 7Hz and 9 samples under 15Hz loading frequency) and also 9 samples were tested under 25 °C with 85% of moisture.

The environmental conditions were simulated in a heat chamber by controlling the temperature and the entry of moisture provided by a Thermotron SE-type 300 conditioner installed next to the MTS machine. An extensometer system camera was used to measure the longitudinal strain on the sample through the window of the thermal chamber during the fatigue testing. This system has been synchronized with the controller of the MTS machine to provide automatic control during fatigue testing. Two high power lights have been used to heat the glass in order to eliminate the condensation that forms on the glass of the thermal chamber during the tests under moisture condition. Two thermocouples placed on the surface of the sample were used to monitor the temperature of the sample during the tests. A hygrometer has also been installed in the room to monitor the level of moisture in the room.

The acoustic emission data acquisition system used during the experiments is provided by Mistras group. The measurement system shown in figure 1 includes four piezoelectric sensors from PAC. The used WD piezoelectric sensors are characterized by a large frequency response band up to 1 MHz which had a maximum sensitivity between 125 kHz and 450 kHz. Each sensor is connected to a preamplifier that transmits analogic signals to an eight-channel acquisition and treatment unit µDISP. The AE signals data are therefore gathered and stored digitally on a computer via a PCI connection bus using *AEWin* software [24-26]. The signal processing, feature extraction, data management and manipulation are performed by *AEWin* Post software. After each test, the AE signals were further analysed using Noesis Software from Mistras. The AE monitoring configuration for damage localization uses four WD sensors is presented by figure 1.

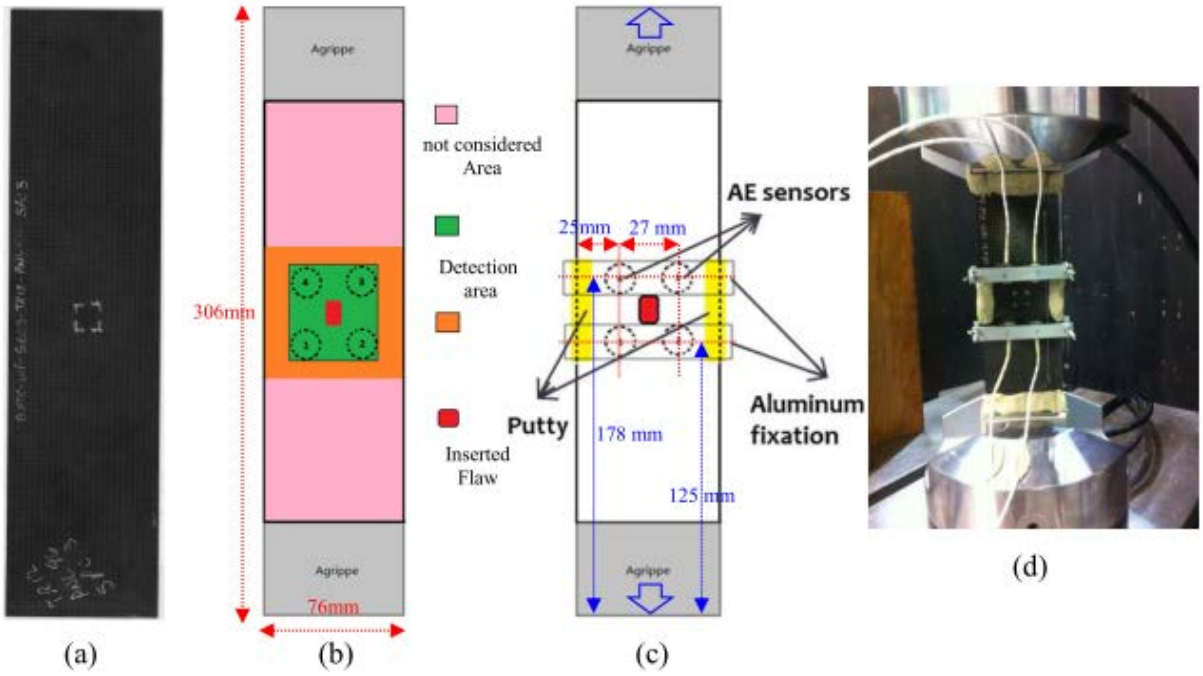

Figure 1: Composite sample with embedded flaw and acoustic emission experimental setup for damage localization around the embedded flaw.

The PZT sensors were positioned at the same distance from the embedded flaw location and

attached to the specimen using fasteners made of aluminum and rubber as a fixture system and acoustically coupled with vacuum grease. This configuration allows using the 2D anisotropic location algorithm provided by the AE apparatus.

The purpose of the localization in the acoustic emission monitoring method is to determine the coordinates of the damaged zone where the acoustic event occurred. The method consists in measuring the difference of the arrival times (Δt) of the same guided ultrasonic wave to several sensors distributed on a structure in order to determine the position of the AE source [26]. Measurement of arrival times (ToA) is triggered by the arrival of the AE wave at the first sensor (First Hit Sensor), and closed by its passage to the last sensor (Figure 2). When the difference in time of arrival of the same guided wave to the different sensors is known, the position of the source of acoustic emission can be calculated by the equations which give the expressions of Δt_2, Δt_3, Δt_4 as shown by Figure 2. Here, Δt2, Δt3, Δt4 respectively, represent the difference in the arrival times between sensors 2-1, sensors 3-1 and sensors 4-1, V represents the velocity of the AE wave propagation in the composite and (x_s,y_s) refers to the coordinates of the position of the AE source.

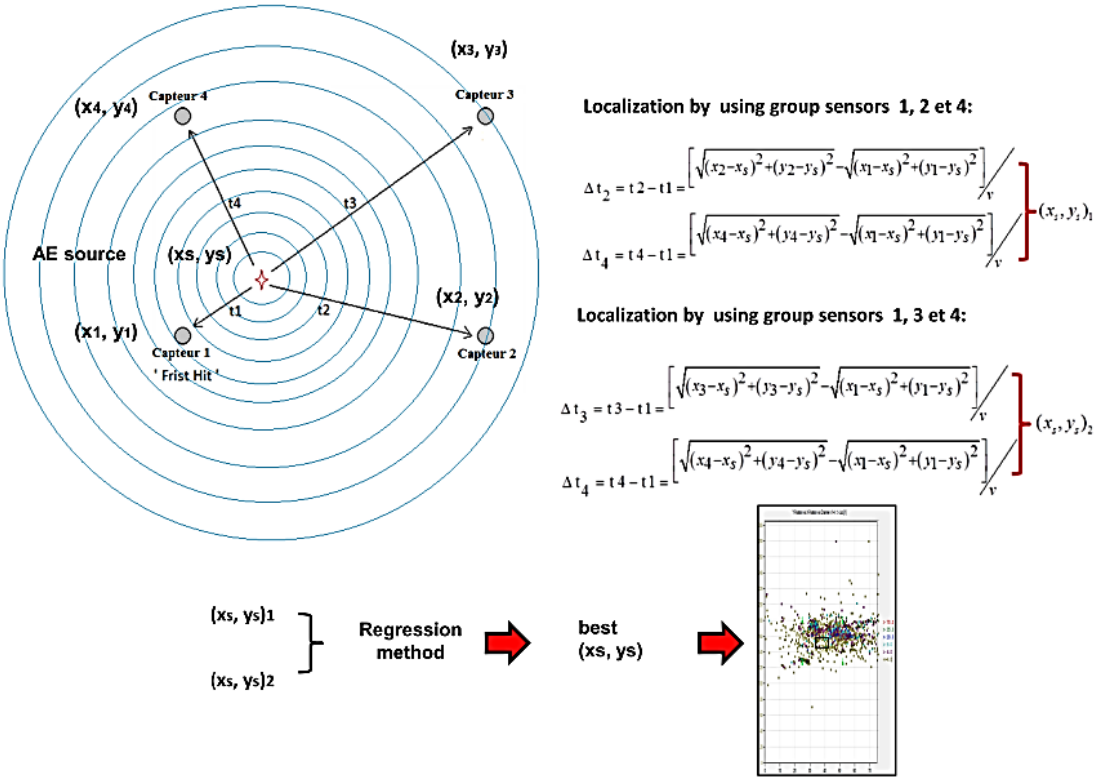

Figure 2: Schematic representation of a planar location approach with four AE sensors

In order to carry out the localization tests, it was necessary to perform guided wave velocity measurements [25] along the two orthogonal directions of a quasi-isotropic composite plate. The velocity value was estimated at 5000 m / s. The velocity was estimated by pencil break tests and was also verified with Laser Doppler Vibrometer, which was used to generate lamb wave dispersion curves for the material. The AE detection threshold was chosen equal to 75 dB for all fatigue tests. Increasing the threshold value intended to reduce the noise caused by the external acoustic sources during dynamic testing. Otherwise, the selected sampling rate was 5 MHz and the system timing parameters were set at 800 µs for HDT (hit definition time), 200 µs for PDT (peak definition time) and 1000 µs for HLT (hit Lock-out time). A filtering interval between 100 kHz and 2 MHz was chosen. The same experimental conditions were adopted for all tests and putty was applied on the grips and around tabs in order to minimize mechanical vibration noise.

3 RESULTS AND DISCUSSIONS

3.1 Damage initiation under static loading

Coupons with embedded flaws and no flaws were submitted to a preliminary quasi-static tension tests to determine the static strength of composites, and also to distinguish the applied stress levels, defined as "Acoustic Emission threshold", from which the coupons generate acoustic emission waves. These stress values indicate the onset of matrix and interface micro-failures in the laminate.

Figure 3 presents the evolution of the cumulative AE counts versus the normalized load applied during a static tensile loading for all tested specimens. The loads were normalized against ultimate tensile load (Load/UTL). Cumulative AE count curves tend to increase exponentially with increasing static load, and follow a similar growth trend for all tested coupons. However, the rate of curves growth is different for each coupon. A range of threshold loads corresponding to damage onset is identified for every tested coupon. The load versus displacement curve representing the normalized failure levels and the static damage onset points is plotted in figure 4.

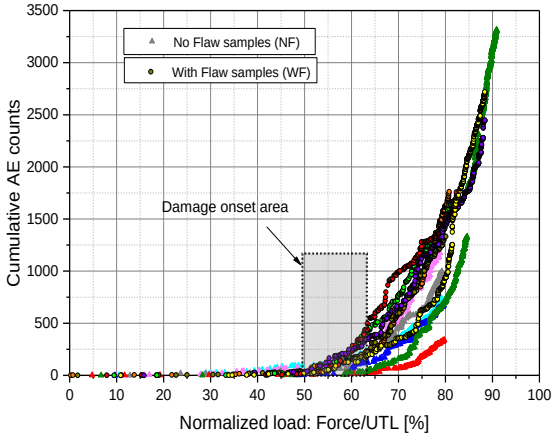

Figure 3: Cumulative counts versus load levels

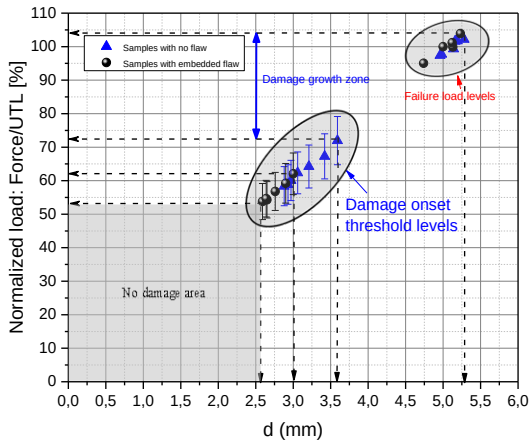

Figure 4: damage onset threshold under static loading

Few differences can be observed between the failure points of samples with flaw (WF) or without flaw (NF). But, the normalized load range for the damage onset is slightly different for the specimens containing embedded flaws (WF), spreading from 53% to 61%, whereas a 58% to 70% range is observed for NF samples of the ultimate tensile load (UTL). Figure 4 displays the no damage zone, in which no acoustic emission activity was detected under static loading. The normalized loading range spreads from 53% to 71% was defined as damage onset zone for both unflawed and flawed coupons. The last zone, corresponding to damage growth zone, appears at between 71% and 102% and testifies of the high growth rate of damage. The results shown in Figure 4, identify accurately; the loading region without damage generation in unflawed and flawed composite coupons; the load levels that were conducive to the creation of the micro-failures in the composite, very likely related to matrix cracking and fiber-matrix interface failure; the loads interval promoting damage propagation associated with macroscopic interface failure and finally, the final rupture load levels of composite coupons, which is characterized primarily by fiber breakage.

3.1 Fatigue life curves

In this work several fatigue tests were carried out with various load levels, in order to study the mechanical behavior of the composite and also to generate fatigue life curves associated with damage initiation, embedded flaw propagation and the total failure of the sample. The acoustic emission method was applied to all tests to detect damage initiation around an embedded flaw using the sensor's configuration presented by figures 1 and 2. The tension-tension fatigue tests were carried out under several environmental conditions: ambient condition, high-temperature condition (82°C and 120°C), a

condition with moisture and condition combining elevated temperature and moisture. The definitions of samples and conditions are described in table 1. In addition, two different cycling frequencies; 7Hz and 15Hz, were applied during cyclic loading to study the influence of the frequency factor into the fatigue life of the samples. The AE source localization method was applied during fatigue tests to locate the emergent damage, in the region around the artificial defect, in order to identify the damage initiation threshold associated to artificial flaw and finally to establish fatigue life curve related to the onset of the propagation of an artificial flaw.The detail of the methodology was presented elsewhere. NDT techniques based on ultrasonic C-scan inspection and X-ray 3D tomography were applied to characterize the damage generated in the samples and around the flaw area.

3.1.1. Effect of cycling frequency on flaw propagation

Ambient temperature fatigue tests were carried out on samples having a flaw inserted at the sample center. Two cycling frequencies were considered; 7Hz and 15Hz. As described in Table 1, five tests were carried out with four loading levels at a frequency of 7Hz, and six tests were carried out with three different loading levels for the case of 15Hz frequency. AE source location analysis, have permitted to detect damage generation around artificial flaw area and helped to estimate the required number of cycles to propagate artificial flaws. The identified thresholds which are related to the damage initiation were used to generate the S-N curves shown in figure 4. In order to emphasize the AE signals that are associated with the propagation of macroscopic delamination, a filtering procedure based on the signal duration and frequencies of AE signal was developed. This AE data filtering method helps to reduce the feature matrix of fatigue data by eliminating data associated with noise induced by fatigue crack opening and closing. The data feature filtering approach was applied for all recorded AE data. Thanks to the use of AE feature filtering, matrix damage onset and delamination onset thresholds have been identified and served to generate fatigue life (S-N) curves based on log-linear straight-line assumption by fitting the experimental points. The models were found by using the following analytical expression $(\sigma/\sigma_{UTS})=a+b.\log(N)$ where, a and b are the intercept and the slope of the curve.

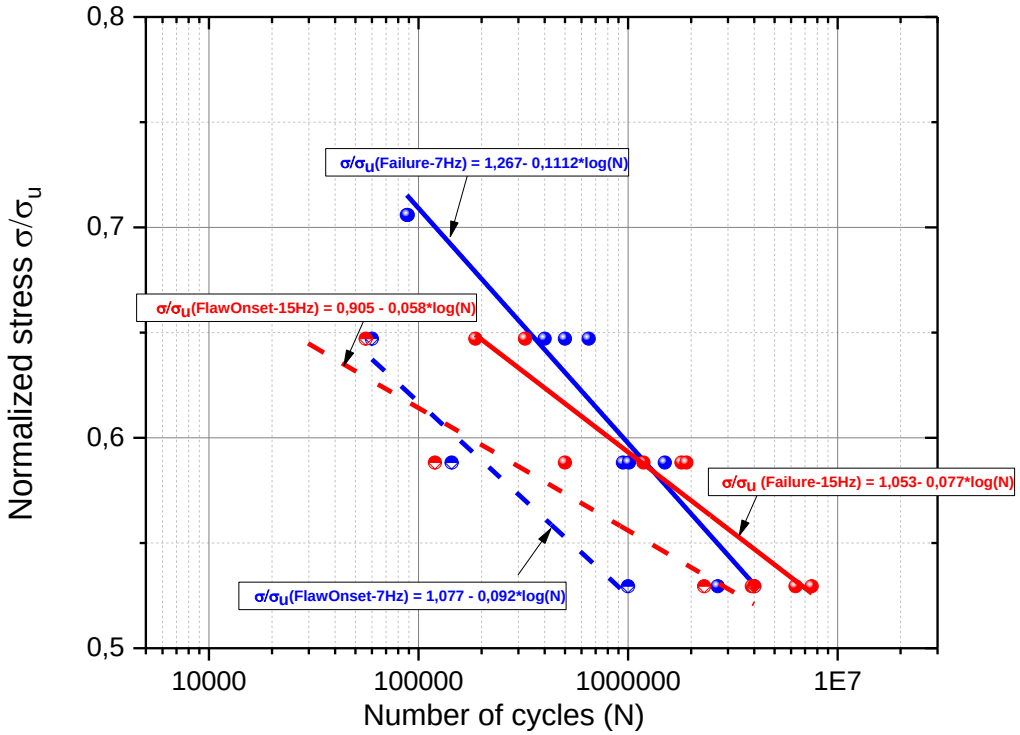

Figure 4 – S/N fatigue life of flaw propagation and failure obtained by AE monitoring and localization data for 7Hz and 15 Hz at RT test cases.

Fatigue models expressed by analytical equations were derived and presented by figure 4. The solid lines represent the S-N curves corresponding to the complete failure of the samples. The dashed line curves correspond to the S-N curves representing the propagation of the artificial flaw obtained by acoustic emission localization technique.
The S-N curves denoted in the figure by $\sigma/\sigma u_{(FlawOnset\text{-}7Hz)} = 1{,}077 - 0{,}092 * \log(N)$ and by $\sigma/\sigma u_{(FlawOnset\text{-}15Hz)} = 0{,}905 - 0{,}058 * \log(N)$, designates the AE fatigue life initiation thresholds, obtained by performing cyclic loading at 53%, 59% and 65% of the ultimate tensile load under 7 Hz and 15Hz. These curves represent fatigue life curves which were associated with delamination onset generated by artificial flaw [9]. Figure 4 shows that the effect of the cycling frequency on flaw propagation is more pronounced for 53% UTL loading case than for the high load's levels such as 59% and 65% UTL. Indeed, under a cycling frequency of 7Hz, the flaw zone becomes acoustically active, when the number of cycles reached 994 714 cycles, against, under the frequency of 15 Hz, the flaw zone is active for the number of cycles as high as 2,361,444 cycles. These results were confirmed by ultrasonic C-scan imaging performed on some selected coupons. Figure 5 shows an example of damage's growth around the embedded flaw obtained by 3D Computed Tomography which has been used to evaluate the damage morphology around the artificial flaw area in the tested coupon. The results were used to compare with the damage localization results obtained by AE technique by planar localization of AE sources during fatigue loading.

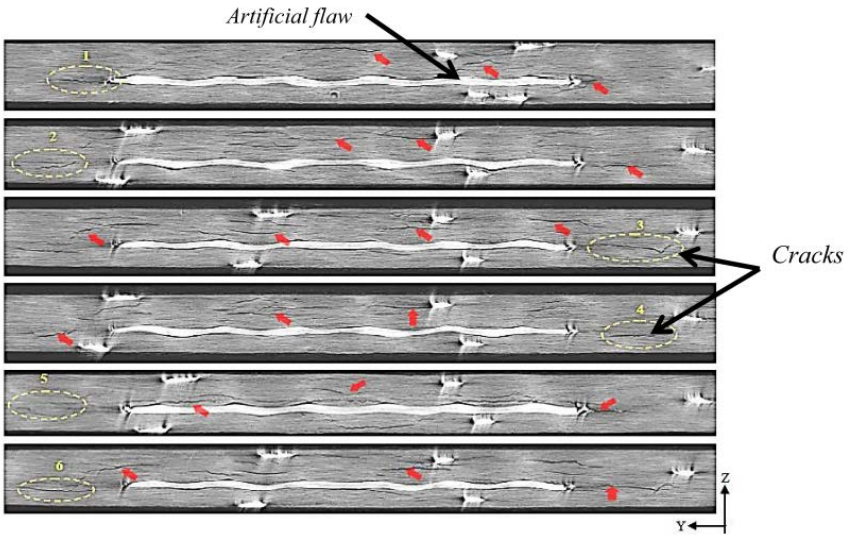

Figure 5 – Fatigue damage distribution around an embedded flaw obtained by 3D Computed Tomography under 15Hz cycling frequency at RT.

3.1.2 Effect of high temperature testing (120^{0}C) on flaw propagation

The purpose of this part was to investigate the effect of thermal degradation of the matrix and fiber/matrix interface on the fatigue life and flaw propagation. The thermal degradation is induced by exposing the composite to isothermal high temperature during mechanical loading. It's well known that the combined effect of environmental and mechanical degradation tends to shorten the fatigue life of composites compared to those that have not been environmentally exposed. Ten coupons were used to perform high-temperature fatigue tests under 7 Hz cycling frequency in dry environment. Ultimate static tensile load was found to be normally lower in a 120°C dry environment than in the room temperature. Tension-tension fatigue testing was done for 53%, 59%, 65% and 71% of the ultimate tensile load obtained by static testing at 120^{0}C. The tests were stopped before final failure when an increase of 5 % of the strain is reached. The strain measurements were performed employing a non-contact strain measurement done by using a high-speed video-extensometer. The AE signal processing technique and the location setup were kept the same as the fatigue tests done under room temperature.

Figure 6, presents the S-N curves results obtained for both cases of fatigue tests conducted under high and ambient temperature conditions. The solid lines represent the S-N curves corresponding to the complete failure (or the 5% strain criterion at 120^{0}C) of the samples. The dashed line curves correspond to the S-N curves which represent the propagation of the artificial flaw obtained by acoustic emission localization technique. The comparison of S-N curves shown in figure 6, displays that the samples having undergone fatigue tests at a 120^{o}C temperature were seriously affected by temperature exposure. To achieve the comparison shown in figure 6, stress data were reduced dividing the maximum stress by the ultimate static tensile stress obtained at room temperature. Figure 6 shows that fatigue lives are significantly lower for the specimen exposed at high temperature than for unexposed specimens. For example, in the case of 59% of UTL loading, initiation of damage around the artificial defect begins at 150 081 cycles, whereas for samples exposed to 120^{0}C, the damage initiation around the artificial defect begins at 7422 cycles which is very early when compared to the behavior of composite samples tested at room temperature. In summary, the obtained results show clearly that the fatigue loading under high-temperature accelerates significantly the process of matrix and the interphase fiber/matrix degradation, which is weakening the composite toughness and promotes early damage of the matrix and the fiber/matrix interface and contribute to the rapid spread of delamination around the artificial flaw.

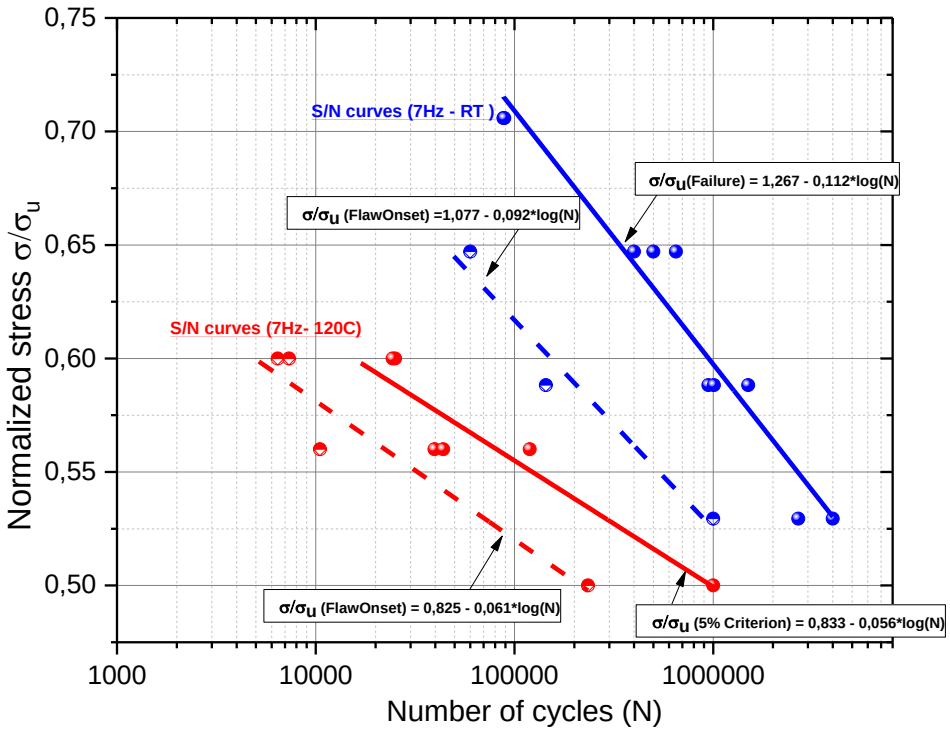

Figure 6 – S/N fatigue life of flaw propagation and failure obtained by AE monitoring and localization data obtained under RT and 120^{0}C test cases for 7Hz cyclic frequency.

3.1.2 Effect of combined action of humidity and temperature

In this section, fatigue tests under different environmental conditions are presented. Two conditions combining temperature and humidity factors were tested in order to study their influences on fatigue behavior and on flaw propagation. The first condition corresponds to an environment evolving at a temperature of 82 °C with a moisture content of 85%. The tests for this condition are carried out with two loading frequencies: 7Hz and 15Hz. These fatigue tests made it possible to study the influence of temperature and moisture as well as the frequency factor. The second condition represents an

environment at a temperature of 25°C with moisture content of 85% and fatigue testing tests were carried out with a loading frequency of 15 Hz.

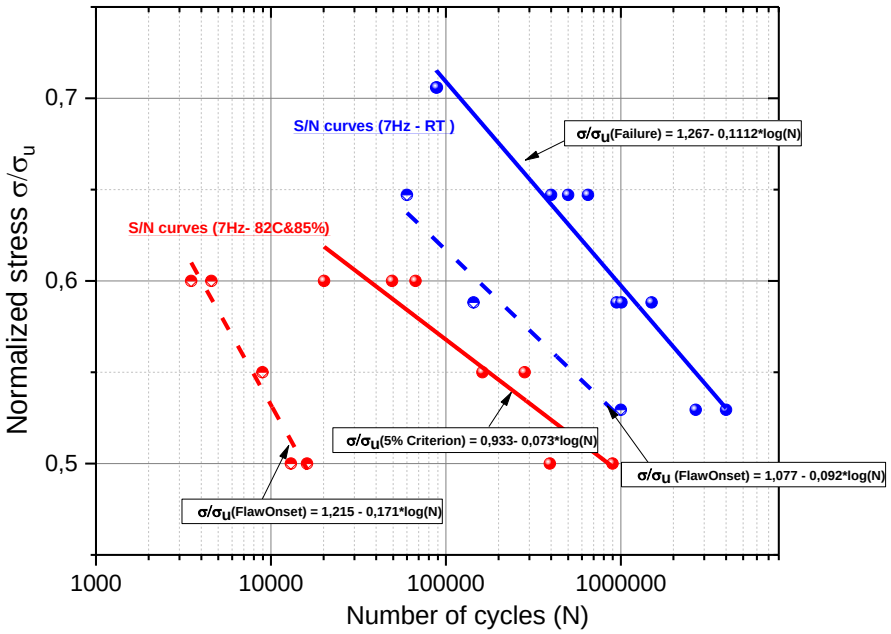

Figure 7 – S/N fatigue life of flaw propagation and failure obtained by AE monitoring and localization data obtained under RT and 82^0C-85% test cases for 7Hz.

Figure 7 presents the results of fatigue tests under 7Hz obtained for samples which have been subject to the condition of 82 °C with a moisture content of 85%. The S/N curves are compared with those obtained during the fatigue test on samples tested at a frequency of 7Hz under ambient temperature condition (RT). This comparison makes it possible to evaluate the influence of the combined effect of temperature and humidity on the generation of damage around the inserted flaw. Again, the solid lines represent the S-N curves corresponding to the complete failure (or the 6% strain criterion for the 82°C & 85% condition) of the samples. The dashed line curves correspond to the S-N curves which represent the initiation of damages around the artificial flaw as detected by AE localization technique. These curves show that damage initiation thresholds for the samples tested under RT condition appear at higher cycle numbers than in the case of samples, which have undergone combined effect of temperature and moisture. For example, in the case of loading of 55% UTL, the threshold of damage occurrence is rated at 521,264 cycles for the samples tested at RT condition; on the other hand, it is only of 8142 cycles when the samples are tested under the condition of 82^0C and 85% moisture. This represents a 98.5% decrease in fatigue life. For the loading case of 60% UTL, the damage occurrence is rated at 148,545 cycles for the samples tested at RT condition and it is only of 3994 cycles when the samples are tested for 82^0C and 85% moisture condition. In this case the decrease in fatigue life is about 97.3%. In general, fatigue loading on samples exposed simultaneously to temperature and humidity stimulate degradation and cracking of the matrix and fiber/matrix interface. From the comparative analysis of the preceding S-N curves, it can be seen that moist aging greatly influences the fatigue life of the samples. When the temperature factor is taken into account, the influence on the S-N curves is strongly accentuated. It can then be concluded that moisture degrades the mechanical properties of polymer matrix composites, diminishes the fatigue life of composites and this reduction is greatly intensified when the sample is exposed to elevated temperatures. Temperature weakens the polymeric matrix of the composite and also promotes diffusion of moisture in laminates, which favors cracking around the defect and accentuates its spread under cyclic loading.

4 CONCLUSIONS

This study uses acoustic emission techniques to generate fatigue life curves for plain weave composites submitted to fatigue tension-tension loading. The objective is to develop an experimental method, which permit to evaluate the influence of manufacturing flaws and environmental factors such as moisture and temperature on the fatigue life. Standards test coupons contained an artificial flaws, which is created by inserting a Teflon tape on the middle plan of the lay up during manufacturing process were tested under fatigue loading.

The development of a monitoring strategy based on the location of AE sources, utilizing four piezoelectric sensors, has allowed generating successfully fatigue life curves. These curves were used to determine the fatigue life corresponding to the spread of delamination from an artificial defect inserted into the material. The generation and comparison of S-N curves under different test conditions helped to highlight the influence upon the cyclic frequency, temperature and the combined effect of temperature and moisture on fatigue life. The following conclusions were reached; first, it has been observed that the increase in temperature greatly reduces the fatigue life of the samples. This effect is caused by the degradation of the matrix at high temperature. The mechanical properties of the matrix become weak, and cracks appear earlier and spread more easily during fatigue testing. Second, the presence of moisture plays a very important role in fatigue life. The moisture absorbed by the samples degrades the mechanical properties of the polymer matrix composite. This deterioration is more important when combining the humidity and the temperature, which favoring the early cracking of the composite and facilitating the propagation of the artificial defect, consequently, the reduction of the fatigue lifetime of the composite. The results also show that the 7Hz S-N curves intersect the 15Hz fatigue life curves. In general, at lower load levels, the 15Hz cycling frequency promotes the fatigue strength of the samples, but when the load level increases, the 15Hz cycling frequency becomes a negative factor which can decrease the fatigue strength of the samples. Finally, the use of 3D X-ray tomography has made it possible to develop an accurate mapping of damage distribution and the propagation scenario of cracks around the artificial defect.

ACKNOWLEDGEMENTS

This work was funded by the Consortium for Research and Innovation in Aerospace in Québec (CRIAQ), Natural Sciences and Engineering Research Council of Canada (NSERC), Bell Helicopter Textron Company (BHTC), Bombardier Aerospace (BA), L-3 MAS Communications and Mitacs. Authors fully acknowledge professor Anh Dung Ngo and his team at École technologie supérieure (ETS-Montreal) for their help on mechanical testing at high temperature. This work present the results obtained during Jiaping Wu his research master program at université de Sherbrooke.

REFERENCES

[1] R. Talreja, "Studies on the failure analysis of composite materials with manufacturing defects" Mechanics of Composite Materials, Vol. 49, No. 1, March, 2013 (Russian Original Vol. 49, No. 1, January-February, 2013).

[2] R. A. Garrett, " Effect of manufacturing defects and service-induced damage on the strength of aircraft composite structures". ASTM International, 1986, pp 5-33.

[3] C. G. Davila," Analysis of the effects of residual strains and defects on skin stiffener debonding using decohesion elements", 44th AIAA structures/ Structural dynamics and materials conference, AIAA 2003, April 2003.

[4] J. Summerscales, "Manufacturing defects in fiber reinforced plastics composites". Insight, December 1994, 36(12), pp 936-942. Composites Structures, vol. 61, pp.333-339

[5] P. A. Carraro, L. Maragoni, M. Quaresimin "Influence of manufacturing-induced defects on the intra-and inter-laminar properties of carbon epoxy NCF laminates". 20th International Conference on Composite Materials, Copenhagen, 19-24th july 2015.

[6] D. Hsu, S. Hair, "Evaluation of porosity in graphite epoxy composite by frequency dependence of ultrasonic attenuation". Review of progress in Quantitative Non-Destructive Evaluation, 6, 1185-1193.
[7] N. J. Pagano and G.A. Schoeppner (2000), "Delamination of polymer matrix composites: problems and assessment ", Comprehensive Composite Materials 2, A Kelly and C Zweben Eds, Elsevier Science, Oxford, 433–528.
[8] T. Tay, "Characterization and analysis of delamination fracture in composites: An overview of developments from 1990 to 2001 ", 2003, Applied Mech Rev, vol 56, no1, January 2003.
[9] T. Tay, F. Shen, "Analysis of delamination growth in laminated composites with consideration for residual thermal stress effects ", Journal of Composite Materials, 36, 36 (11) (2002), 1299-1320.
[10] M.N. Bureau, J. Denault, " fatigue resistance of continuous glass fiber polypropylene composites: temperature dependence ". Polymer Composites, 25, 622-629.
[11] I. Silversides and A. Maslouhi (2010); "Determination of interlaminar crack initiation criteria envelope in composite materials using acoustic emission monitoring", Eighth Joint Canada-Japan Workshop on Composites, July 26-29, 2010, Montreal, Canada.
[12] P. L. Braisaz, N. Kanouni and A. Maslouhi, Characterization of fatigue delamination growth from embedded flaw in plain weave composites by using hybrid monitoring approach. Submitted paper for the journal of Structural Health Monitoring, January 2015.
[13] N. Kanouni, J. Wu, A. Maslouhi and P. Braisaz, " Assessment of fatigue damage onset and growth in plain weave composites with embedded flaws" 20th International Conference on Composite Materials, Copenhagen, 19-24th July 2015.
[14] J. Degrieck, W. Van Paepegem, "Fatigue damage modelling of fiber –reinforced composite materials: Review ", Applied Mechanics Reviews, 54 (4) (2001), 279-300.
[15] S. Wicaksono and G. B. Chai (2012). A review of advances in fatigue and life prediction of fiber-reinfoeced composites. J Materials: Design and Applications, vol. 227 (3). pp.179-195
[16] R. Khan, Z. Khan and al., Fatigue life estimates in woven carbon fabric/epoxy composites at non-ambient temperatures, Journal of Composite Materials, 36, 2002, pp. 2517-35.
[17] S. Wicaksono and G. B. Chai. A review of advances in fatigue and life prediction of fiber-reinforced composites, Journal of Materials: Design and Applications, 227, 2012, pp. 179-195.
[18] T. Osada, A. Nakai, H. Hamada (2003). Initial fracture behavior of satin woven fabric composites, Composites Structures, vol. 61, pp.333-339.
[19] K. Ono and A. Gallego, Research and application of AE on advanced Composites, 30th European Conference on Acoustic Emission Testing & 7th International Conference on Acoustic Emission, Granada, Spain, September 12-15, University of Granada, 2012.
[20] M. Surgeon, M. Wevers M.,"Modal analysis of acoustic emission signals from CFRP laminates". NDT&E Int 1999;32:311–22.
[21] M. R. Gorman and W. H. Prosser (1991), "AE Source Orientation by Plate WaveAnalysis" Journal of Acoustic Emission, 9(4), 283-288.
[22] M. R. Gorman (1990), "Plate Wave Acoustic Emission," J. Acoust. Soc. Am., 90(1), 358-364.
[23] S. Barré, M.L. Benzeggagh (1994). On the use of acoustic emission to investigate damage mechanisms in glass-fibre- reinforced polypropylene. Composites Science and Technology. vol. 52, pp.369-376
[24] I. Silversides, A. Maslouhi and G. Laplante; "Acoustic emission monitoring of interlaminar delamination onset in carbon fibers composites", Structural Health Monitoring; 12(2): 126-140, 2013.
[25] A. Maslouhi and R. Cherif (2009); "Fatigue damage monitoring in adhesive joint by using guided waves" American Society for Composites-24th Technical conference, hosted by C. for compo. Mat. (U.of Delaware), edited by J. W. Gillespie and S. V. Hoa, ISBN 978-1-60595-008-2.
[26] MISTRAS Group Inc., Products & Systems Division, Princeton Junction (2011). AEwin software, Installation, Operation and User's Reference Manual. New Jersey, USA.